Aerostatic thrust bearings active compensation: Critical review

Aerostatic Thrust Bearings Active Compensation: Critical Review

Terenziano Raparelli, Vladimir Viktorov, Federico Colombo, Luigi Lentini*

Department of Mechanics and Aerospace, Politecnico di Torino, Corso Duca degli Abruzzi 24, 10129 Turin, Italy

Abstract

Aero-static thrust bearings are widely used in high precision conventional applications, e.g., in machine tools, measuring instruments, precise positioning systems, manufacturing and medical equipment. Their appeal is due to the absence of contact between moving and stationary parts, which ensures their low friction, limited heat generation and long life. Moreover, the use of air bearings usually do not contribute to the environmental contamination.

However, aerostatic thrust bearings have usually lower stiffness and load capacity than rolling or oil bearings. For this reason, active and passive compensation are currently used to enhance these properties, thus extending the bearing's operating range. Recently, active compensation methods have become more popular thanks to improvements in mechatronics technology, and because they can provide the very high accuracy required by current high precision applications. This paper reviews the state of the art of the active compensation method and provides general classification criteria, outlining dissimilarities and the pros and cons of the available solutions.

The paper concludes with several considerations and comments regarding the main performance features of each solution.

*Corresponding author FAX:+39-0110906999 ; TEL: +393481645062; luigi.lentini@polito.it

Email addresses: terenziano.raparelli@polito.it (Terenziano Raparelli), vladimir.viktorov@polito.it (Vladimir Viktorov), federico.colombo@polito.it (Federico Colombo)

Keywords: air thrust bearing, active bearings, high precision support.

Nomenclature

$A(\Omega)$	Actuator transfer function
$C(\Omega)$	Controller transfer function
$e_H(\Omega)$	Controller height error
$e_h(\Omega)$	Air gap thickness error
F_0	Static applied load
$\bar{F}$	Dimensionless load capacity indicator
F_∞	Maximum bearing load capacity for obtaining infinite stiffness
$F(\Omega)$	External dynamic load
$F_c(\Omega)$	Bearing thrust force
$G_m(\Omega)$	Transfer function of the supported mechanical system
$G_{P/h}(\Omega)$	Air gap transfer function
$G_c(\Omega)$	Air flow control transfer function
h_0	Air gap thickness initial value
$h(\Omega)$	Air gap thickness
h_{Ref}	Air gap height reference value
h_T	Measured air gap height
H_0	Controlled height initial value
$H(\Omega)$	Controlled height
H_{Ref}	Controlled height reference value
H_T	Measured controlled height
$K = -\frac{\partial F}{\partial h}$	Air bearing static stiffness
$K_{F/P}$	Static gain (active bearing surface)
$P_c(\Omega)$	Air gap pressure distribution
$\bar{P}_c(\Omega)$	Modified air gap pressure distribution
P_{mean}	Mean value of the air gap pressure distribution

P_s	Supply Pressure
Q	Air flow consumption
R_{gap}	Air gap flow resistance
R_{in}	Internal flow resistance of the bearing
$T(\Omega)$	Transducer transfer function
S	Active Bearing surface
$u(\Omega)$	Manipulated variable
Z_0	Air Pad initial thickness
$Z(\Omega)$	Air Pad thickness
Ω	Frequency

Table 1: List of Symbols

Acronyms

AIR	Active Inherent Restrictor
ATB	Aerostatic Thrust Bearing
ECR	Exhaust Control Restrictor
PID	Proportional Integrative Derivative
PZT	Piezoelectric actuator

Table 2: List of Acronyms

1. Introduction

Conventional Aerostatic Thrust Bearings (ATBs) are widely used in high precision applications, e.g., in machine tools, measuring instruments, precise positioning systems, manufacturing and medical equipment, etc.

A schematic representation of a conventional ATB is shown in Figure 1, where 1 is the moving pad and 2 is the stationary part. Air at pressure P_s is supplied

through a restrictor (whose resistance is denoted by R_{in}) into the gap between the pad and the stationary part of the bearing. The air is then exhausted to the atmosphere through the gap's distributed resistance R_{gap}. In this way, the pressurized air in the clearance is able to support the external load F. P_{mean} is the mean value of the air clearance pressure distribution P_c, h is the air gap height, Z is the thickness of the pad and H is the sum of the gap height and pad thickness. If the external load increases (decreases), the resistance of the air gap increases (decreases) and the pressure distribution in the clearance increases (decreases), thus balancing the external load again. The main advantages of these bearings stem from the absence of contact between moving and stationary parts which makes it possible to achieve very precise positioning and excellent start up performance, as there is no stick-slip. Moreover, a clean environment can be preserved thanks to the absence of oil lubricants, and heat generation is very low under operating conditions. All these advantages allow maintenance to be limited, reducing system downtime and the associated costs.

Air bearing performance (stiffness, damping, load carrying capacity, flow rate and stability) is closely related to the feeding restrictor adopted, which can be of several types, e.g., pocketed or unpocketed orifice, elastic orifice, restricting land, capillary slot, porous surface, etc. All of these technical solutions bring particular prons and cons [1]. The literature presents many studies about these feeding devices. In [2], Belforte et al. computed discharge coefficients for different types of orifices for aerostatic bearings are analysed, whereas M. Fourka and M. Bonis in [3] produced a valuable analysis by comparing optimum characteristics of different kinds of orifices and feeding systems. Nowadays, the improvement of load capacity and both static and dynamic stiffness, in absence of instability, represents the majority of the research on gas bearing design. In designing air bearings, the static characterization represents the first step of the procedure. The air consumption Q, the bearing force F_c and the static stiffness $K = -\frac{\partial F}{\partial h}$, expressed as functions of the air gap width h, for a given supply pressure P_s and bearing size, asses the static performance of a gas bearing.

It is worth pointing out that infinite static stiffness (around a working point) means that small changes in the bearing load will leave the gap unaltered at almost zero frequency. Concerning aerostatic thrust bearing performance, it has been demonstrated by many authors ([4], [5], [6]) that, especially for small air gap values, bearings with convergent gap geometries yields higher load capacity, stiffness and dynamic stability. The air bearing dynamic characterization is usually the second design step. In this phase a characteristic instability phenomenon have to be taken into account, the so called "pneumatic hammer". This phenomenon is due to the air compressibility and the consequent delay between bearing clearance changes and pressure variation in it [7]. It was found that pneumatic hammer is governed by the geometry, supply pressure and the load applied to the bearing, whereas it is largely independent of relative tangential speed of the bearing surface [8]. In enhancing gas bearing performance, care must be taken to pneumatic hammer, because, its likelihood seems to increase as one tries to improve the static characteristics [5]. Compensation systems are currently adopted in order to extend the gas bearing range of application. The literature presents many compensation systems examples. They were designed either embedded in the pad or external to it depending on the considered application and on the gas bearing size. There are two main kinds of compensation: passive and active compensation. In passive compensation, performance improvements are achieved without adding energy than that resulting from the bearing supply air, using only passive devices. On the other hand, in active compensation, external actuators are used to modify the gas bearing behaviour.

Passive compensation generally is not able to achieve infinite stiffness. Nevertheless, there are some peculiar solutions in which infinite stiffness is obtained, avoiding instability, over more than 20% of the bearing load range [9] and up to a bandwidth of 5 Hz. These solutions exploited the shape variation of the bearing gap to compensate for load changes. A flexible convergent membrane was incorporated in the air bearing as the active surface. This membrane allows external load variations to be compensated by the conicity changes. When a load variation occurred, the membrane deflected in such a way to create a new

pressure distribution in order to restore the static equilibrium of the bearing.

In order to analyse the stability of externally pressurized bearings, it can be valuable to represent the ATB as a closed loop servo system as shown in Figures 2(a) and 2(b). In this kind of closed loops, it is possible to identify the passive (direct branch) and the active (feedback branch) bearing functions which represent the supported mechanical structure and the influence of the gap variation on the thrust force respectively [8], [10]. Here, transfer functions and variables are expressed in the frequency Ω domain. Figure 2(a) represents the closed loop servo system of a conventional bearing. Where, the input of the bearing systems (Figure 2(a)) is the external load variation $\Delta F(\Omega)$, the output corresponds to the air gap width variation $\Delta h(\Omega)$. $G_m(\Omega)$ is the transfer function of the supported mechanical system, $G_{P/h}(\Omega)$ is the air gap transfer function and $K_{F/P}$ is the static gain which links the air gap pressure to the load capacity. The general closed loop of a passive compensated gas bearing is sketched in Figure 2(b), where the transfer function $G_c(\Omega)$ embodied the passive compensator device (or mechanism). A variety of investigations have been carried out to develop this kind of systems. R.Snoeys and F. Al-Bender in [5] presented a methodology for improving the performance of a thrust bearing with a convergent gap. Bryant et al. [9] and Holster et al. [11] designed aerostatic thrust bearings with flexible membranes and convergent gap achieving infinite stiffness and load compensation respectively. Ming Fei et al. [12] developed an X-shaped groove aerostatic bearing with passive disk-spring compensator providing high dynamic performance. Unfortunately, passive compensation methods make it possible to obtain only systems with a low bandwidth.

Nevertheless, these methods are widely used because of their cheapness and ease of integration. As mentioned earlier, bearing performance can also be improved by adopting active compensation system. In such systems, external actuators are used to affect the bearing behaviour. The main prons and cons of active and passive compensation methods are reported in table 3. This paper reviews some of the existing active compensation methods for ATBs presented in the literature and classifies them on the basis of their operating principles. In

view of the fact that active compensation is still not widely used for ATBs, the active compensation designs for journal bearings that can be readily extended to ATBs will also be reviewed. The classification is also very valuable, as the literature contains no publications and references on this subject.
The paper concludes with several considerations and comments regarding the main performance features of each method.

2. Active Compensation methods

After giving the basic definitions, we will deal with the other important topic of the paper, i.e., the active compensation classification criteria.
Currently available compensation methods can be classified in three main categories on the basis of which is the variable controlled by the actuators.

It is possible to distinguish among:

1) " **Active flow resistance compensation method**",

2) "**Active geometrical compensation method**" or

3) "**Hybrid active compensation method** ".

In the first instance, actuators are used to control the opening of restrictors. It is worth noting that the stability of this kind of compensation is dependent on the distance from the air bearing active surface to the restrictor/s [13]. In the second instance, the load compensation is achieved by modifying aspects of the bearing geometry, e.g., the bearing thickness and the shape of the bearing gap. Hybrid active compensation is a combination of the two previous kinds of compensation. This preliminary categorization is rather academic and it have been introduced to organize the present review better.

A further and more useful sub-categorization on these active compensation methods can be done depending on which type of actuator is integrated for the designed application. With the actuators currently used for active compensation flow resistance variations can be achieved by means of:

* Piezoelectric-actuators (PZT)

* Magnetostrictive materials

* Electromagnetic fields

* Pneumatic valves

Since each type of actuator has different characteristics (dynamics, energy density ratio, etc), a table for performance comparison is presented (see Table 6 [14]). It is worth noting that table information are indicative, due to the large amount of existent actuator types for any single class.

As for passive compensation systems, Figures 3 and 4 depict the equivalent closed loop servo systems of the active flow resistance compensation and the active geometrical compensation methods respectively. The main difference between active and passive compensation is the presence of external transducers $T(\Omega)$, actuators $A(\Omega)$ and a controller $C(\Omega)$. In the active compensation, transducers measure the variable of interest ($\Delta H(\Omega)$ or $\Delta h(\Omega)$) and sent this value into the controller which compares it with a set-point value ($H_{Ref}(\Omega)$ or $h_{Ref}(\Omega)$). The actuator input $u(\Omega)$ is generated by the controller depending on the difference between the measured actual value ($H_{meas}(\Omega)$ or $h_{meas}(\Omega)$) and the correspondent set point. For the controller selection, PID controller can be adopted in presence of small disturbances, e.g., precision applications, whereas they have to be designed ad hoc for more general applications.

The performance of some of the reviewed solutions (when data are available) is assessed by comparing a dimensionless indicator of the bearing load capacity $\bar{F}$ and the bandwidth f_{max} of the analysed system.

$$\bar{F} = \frac{F_\infty}{P_s \cdot S \cdot \frac{h}{h_0}} \tag{1}$$

where S is the bearing active surface, h_0 is a reference value of the air gap height (considered equal to 10 μm), F_∞ is the maximum gas bearing load capacity for obtaining an infinite stiffness, h is the correspondent air gap width and P_s the supplied pressure.

3. Discussion on active compensation methods

3.1. Active flow resistance compensation methods

The first method owes its name to the fact that, in order to restore the initial value of the air gap h, it is necessary to control the flow resistance of active restrictors by means of actuators. Controlling the opening restrictor makes it possible to impose a new pressure distribution necessary to compensate for load variations and therefore restore the initial value of H. The active flow resistance compensation method can be broken down into three further subcategories on the basis of the active restrictor position with respect to the air gap position. On the base of this, one can distinguish among:

- Upstream active restrictors
- Air gap restrictors (on the active bearing surface)
- Exhausting restrictors

3.1.1. PZT Actuators

There can be no doubt that piezo actuators are now one of the most widespread technologies in nano and micro precision applications, thanks to the major advances that are being made in smart material actuators. Nierzrecki et al. [15] present a review of piezoelectric actuation, citing different kinds of methods and applications. PZT actuator's large appeal lies in their high mechanical energy density: they make it possible to achieve ten times the energy-mass ratio of conventional actuators (e.g., hydraulic, pneumatic or electromechanical).

In addition, they can generate high displacement and force through a broad frequency range without consuming a significant amount of electrical power.

However, as they have a shortcoming involving their mechanical stroke (the typical free strain induced in these elements is under 0.2%), some amplification techniques are required.

The simplest and most common amplification method is achieved by stacking up thin pieces of piezo ceramic material (internally leveraged)[15]. This

allows their stroke to be linearly increased and the equivalent actuator can be considered as a series of PZT connections (the total stroke is the sum of each one). This section presents a number of active compensation designs with PZT actuators.

For each active compensation architecture, a performance assessment is given by one dimensionless parameter $\bar{F}$ and the system bandwidth.

Some details on control and sensors are also given in order to clarify the system's working principle and to illustrate innovative new equipment.

Exhausting restrictors H.Mizumoto et al. [16], [17] presented an active restrictor which allowed the flow exhausted from the bearing to be controlled, avoiding air hammer and achieving infinite stiffness. Here, the exhaust control restrictors were radially integrated in an air bearing spindle (see Figure 5). A magnified view of the system is shown in Figure 6(a). The ECR consists of a PZT, a spacer, a steel ball, an adjustable screw and a diaphragm. The diaphragm is deformed through the steel ball, moved by the PZT action. The adjusting screw establishes the diaphragm's initial position.

As illustrated in the air bearing section view, the air is divided into outer and inner flow. The ECR was placed in the bearing inner exhaust channel, and can be schematized as a variable flow resistance (see Figure 6(b)). When the external load increased, the ECR's size was reduced by the PZT action and the pressure on the bearing surface could be increased without reducing the air gap. The air gap variation was sensed by electrical micrometers; an appropriate voltage was computed by a microcomputer and supplied to an amplifier which drove the piezoelectric actuator. Here, two ECRs were embedded in a radial bearing with a length of 112 mm and a diameter of 40 mm. The authors stated that, in presence of a supply pressure of 0.49 MPa and an air gap width of 10 μm, the aerostatic spindle showed infinite stiffness up to 70 N loads. In this application the system bandwidth in the radial direction was 50 Hz.

Up-stream restrictors In [18] and [19], Morosi et al. presented an active control for an hybrid gas lubricated journal bearings (see Figures 7(a) and 7(b)). Radial injection of lubricant was regulated by means of piezoelectric actuators mounted on the back of the bearing sleeves. Belleville washers were used to provide the necessary restoring force to the sleeve. Figure 7(a) shows a magnified view of the injection system. To minimize air losses, an O-ring was bonded to the lower surface of the pin. The strain of the PZT allowed the air gap pressure to be modified without changing the shaft position by means of an upstream flow resistance variation. A mathematical model was introduced, for coupling the rotor bearing system dynamic with the mechanical and fluid dynamics of the actuator. In this model, the control was achieved through a simple proportional-derivative feedback low. Simulations showed that this kind of bearing offered considerable advantages compared to conventionally lubricated bearings, not only bringing a considerable reduction of the synchronous vibration component, but also extending the bearing range of application. Moreover, the authors stated that this kind of bearing offers an improved transient response characteristic.

Air gap restrictors In [20], [21] Mizumoto et al. presented a different smart active compensation method which employed a PZT with a through hole, called active inherent restrictor (AIR). By controlling the PZT stroke, it was possible to change the orifice area depth h_d (see Figure 8(a)) independently of the pad air film thickness, and thus obtain a variable pressure distribution under the pad. When the applied load increased, the air gap pressure was also increased by reducing h_d , thus restoring the system's equilibrium without changing the value of gap h. AIRs and other conventional restrictors were installed in an air bearing spindle both in the radial (journal bearing) and axial directions (ATB). The air bearing spindle consisted of a pair of thrust bearings and a radial bearing. Figure 8(a) shows the bearing active surface of the thrust bearing. This surface presents six restrictors with an outlet hole of 0.3 mm diameter and, only in the upper bearings, three of them are AIRs. The outer

and the inner diameters of the thrust bearing surface are 65 mm (D_o) and 30 mm (D_i) respectively. In the same Figure 8(a) a cross section of active inherent restrictor is shown. The radial bearing presented two rows with six of the previous types of inherent restrictors. In each row three of them were AIRs. The inner diameter and the width of the radial bearing surface were 29 mm and 50 mm respectively. The air gap width and the supply pressure were 10μm and 0.49 MPa respectively both for the journal and thrust bearings. Nine capacitance transducers with 10 nm resolution were incorporated to detect the working point displacement (with respect to the Reference ball see Figure 8(b)) both thrust and radial displacements of the spindle. Experimental results showed that the static thrust stiffness of the spindle was much improved and virtually infinite when the load was less than 60 N. In the radial direction, the static stiffness could also be infinite by using AIRs, but with a maximum load of 2 N at most. Authors stated that the spindle bandwidth were 50 and 100 Hz in axial and radial direction respectively.

3.1.2. Magnetostrictive Actuators

Air gap restrictors Terfenol-D is another type of material that can be employed for active compensation. It is a strong magnetostrictive material, and its name comes from the metallic elements terbium (TER), iron (FE), Naval Ordnance Labs (NOL), and Dysprosium (-D). It is characterized by a power energy density with the same order of magnitude of piezoelectric actuators [14] and allows non contact actuations. However, it is very expensive and its magnetic coil is bulky. Further information on Terfenol-D is given by Zhu Houqing et al. [22] in their review. K.Y.Huang and Y.C.Shiao [23] presented a magnetostrictive actuated restrictor making use of this kind of material. In this design, a slot restrictor (see Figure 9) was used to vary the pad's main air restrictor flow.

The movable restrictor pad (see Figure 9(a)) had a diameter of 1.5 mm, the orifice was 5 mm long with a diameter of 1.5 mm. The rotor was made of aluminum alloy with a diameter of 60 mm, the air-film thickness h_c had a

variation range between 10 and 30 μm. The aerostatic bearing was supplied with air pressure P_s ranging from 0.3 to 0.6 Mpa. In order to control the dimension of the restrictor gap h_r, the magnetostrictive actuator was connected to the restrictor core by means of a leverage consisting of flexure hinges to ensure that there was no friction and mechanical losses (see Figure 9(b)). The restrictor core was linearly guided by two parallel spring-sheets.

When there was an increasing load on the system, the restrictor gap h_r was modified by increasing the driving current to maintain a constant air gap h_c. As the driving current was increased, the restrictor gap h_r expanded in turn to augment the air flow rate in the air film h_c and consequently enhance the air gap pressure distribution and thus the load capacity. The figure 10 showed the influence of the driving current and supply pressure on the load capacity air film thickness of 10 μm. Given a supply pressure of 0.6 MPa, the aerostatic bearing achieved the maximum compensation load range between 124.3 and 167.3 N, a load compensation rate (load compensation range/ driving current) about 21.5 N/A generated by restrictor. Experimental results showed that the load capacity was proportional to the driving current.

3.1.3. Electro-magnetic Actuators

Air gap restrictors As mentioned above, electro-magnetic forces can be employed for active compensation.

Unfortunately, as has also been pointed out, large spaces for coils and permanent magnets are needed in order to generate suitable control magnetic forces. In addition, as discussed in [24], the use of magnetic suspension presents many limitations such as losses, saturation and hysteresis. For this reason, such actuators are used in bulky industrial applications.

S.Roa et al. [25] presented an active compensation method for compensating the motion error of a linear air bearing stage through an active magnetic preload (see Figure 11).

A single-axis linear stage was designed with four magnetic actuators attached at the corners of the table in the vertical direction (see Figures 11(a),11(b),

11(c)). The load capacity and stiffness of an air bearing with porous pads were calculated using a numerical method, and a magnetic circuit model was derived for the magnetic actuators. An active feedforward compensation for motion errors in the vertical and pitch motion directions was used. Eight aerostatic porous bearings were located under the table (see Figure 11(b)) to support it vertically and were preloaded by four magnetic actuators attached at the corners, while four bearings were located on each side of the stage. Each of the magnetic actuators consisted of a permanent magnet that generated a nominal magnetic flux for the required preload force and a coil for varying the magnetic force and thus adjusting the air bearing clearance. In figure 11(d) the system specifications are summarized. The vertical stiffness of the table was assessed by applying small forces and measuring the vertical displacement. When the specification conditions were applied to the system (see Figure 11(d)), the difference between the numerical model and experimental results was less than 5%. The authors stated that, in presence of a lower supply pressure and higher magnetic preloads, the vertical stiffness increased due to the smaller clearance. However in these cases the difference between numerical analysis and experimental results showed higher error in the stiffness calculation. At 0.4 MPa supply pressure with a 0.5 mm air gap at the magnetic actuators, a vertical stiffness of 34.4 N/μm was achieved with an air gap width of 13.7 μm.

3.1.4. Valves

Pneumatic valves are another type of actuator used in AC. The main advantage of using this pneumatic actuator stems from its cheapness and ease of integration.

There are several commercially available types of pneumatic valve. Further information can be found in [26].

Upstream restrictors The control scheme of a very simple application patented by G.Russell is shown [27] in Figure 12. Here, a regulating valve was used to vary an up-stream flow resistance (this active control can be classified as

an upstream flow resistance variation method). The air pad (28) was supplied by an electrically controlled compressor which delivers air flow to an air tank (32) through a monostable regulating valve (35).

This active control system was employed in coordinate measuring machines with the aim of reducing air consumption during the period of non-use.

Air gap restrictors An active compensated system using pneumatic valves is presented in [28],[29] (see Figure 13 and 14). This method was used to improve the performance of a pneumostatic journal bearing (Figure 14). The journal bearing had a diameter and an axial length of 30 mm and 60 mm respectively. The bearing incorporated four symmetrically and circumferentially placed orifices with 0.4 mm diameter. In active operation up and down diameters of the inlet orifices were increased till 3 mm while lateral ones were unchanged. These orifices supplied four pockets with mean depth $h = 50$ μm, width a =15 mm and length $L_p = 44$ mm. In nominal condition, the air gap width δ was 20 μm. The control system was shown schematically in Figure 13(a). The control was based on a pressure differential between a reference value p_{rif} and the pressure measured by means of a back pressure displacement transducer $p_{s,T}$ on the up ($p_{P,up}$) and down ($p_{P,down}$) shaft surface. On the basis of the actual pressure differential ($p_{P,up}$-$p_{P,down}$), three diaphragms (1, 2, 3) (Figure 13(b)) positively connected to moving body (7) allowed the downstream pressure to be adjusted by modifying the output flow resistance of the valve from (10). Springs (11) and (12) provided a suitable axial stiffness to the system, while screw (14) was used to regulate the nozzle position. As can be seen from the functional schematics of the closed loop control system shown in Figure 13(a), an approach of this kind could also be readily employed in a thrust bearing. It should be noted that valves act both as actuators and control units, so that application costs are significantly reduced. The authors stated that, this pneumatic active control system allowed the ATB to achieve an infinite static stiffness up to an external load of about 200 N (with a 6 bar supply pressure). In this range the stiffness was ten times greater than the stiffness of the passive case. Moreover, when a

negative step of 50 N was imposed in the vertical direction, the new controlled system recovered the initial position after about 0.5 seconds.

3.2. Active geometrical and hybrid compensation methods

As mentioned before in section 2, the active geometrical compensation method uses actuators to modify the ATB geometry, e.g., the bearing thickness Z and the air gap shape, in order to compensate for load variations. On the other hand the, third possibility is to adopt hybrid compensation systems, where active flow resistance and active geometrical compensation methods are simultaneously used. Until now, according to our knowledge, these compensation methodologies have been used only in one aerostatic thrust bearing prototype. For this reason, both active geometrical and active hybrid compensation methods are considered both in the present section.

3.2.1. PZT Actuators

Figure 15 shows a sketch of the presented active aerostatic bearing, designed by F. Al-Bender et al. [4], [30], [6]. The prototype consisted of a thin plate, with a central air feed hole, which was clamped centrally onto a cylindrical column that connected to the back of the bearing. The deflection of the plates was controlled by three circumferentially and symmetrically placed stack piezoelectric actuators. In this way, when the actuators extended, the active bearing surface deformed to a concave shape. The induced deflection produced a pressure air gap distribution variation and therefore, a variation in the bearing force. This type of active air bearing represent a complex mechatronics system where the final performance depended on different physical phenomena. For this reason, the authors proposed a multiphysics model that combined models for fluid-dynamics, structural flexibility, piezoelectricity and control, with a strong couple formulation. Figure 16 shows a scheme of the active bearing system considering the layout and the block diagram of the active compensation system. In the figure 16, on the left side, all the different possibilities of controlling the active bearing are listed. For the purpose of active compensation, the aerostatic

bearing system incorporated one or a combination of active elements, namely: support and conicity actuators and a supply pressure controller. These introduced an active bearing force. Figure 17 shows the bearing force response to variation in air gap height, conicity and their combination. These results were obtained for a bearing with a diameter of 80 mm, a 1.4 mm feed-hole, a 3 μm conicity, supply pressure of 0.6 MPa, a nominal gap heigth of 10 μm and a PI controller. From here, the hybrid compensation (the combination of the gap and conicity variation) resulted far superior with respect to the other two, taking into account the practically constant gain, the negligible phase shift and the wider bandwidth. After this, an optimization analysis of the system was performed [6]. From this, it was found that the static load carrying capacity of the bearing depends on the amount of conicity and the plate compliance: a positive conicity (concave recess) significantly increases the load that can be carried. The mechanical stiffness of the plate showed two different and opposing effects: on the one hand, lower stiffness allows higher piezo elongation to be achieved, thus obtaining a better compensation. On the other hand, it leads to deformation of the bearing surface due to air pressure which reduces the conicity and hence the load capacity. These experimental results were achieved for two bearings with diameters of 80 mm, a supply pressure of 0.6 MPa, and 6 (thin) and 10 mm (thick) plate thickness respectively. the piezo actuator input voltage varied from 0 to 100 V. Passive dynamic tests were carried out in presence of 300 and 600 N loads. By comparing the performance of both the prototypes (thin and thick), for low static loads, the thin bearing offered slightly higher stiffness, due to the higher conicity induced by the piezos. On the contrary, for high load, the deformations of the pad under pressure was dominant and the thick bearing had higher stiffness. As a final test for the validity of the model the active performance of the bearing was evaluated in presence of a PID controller. In this case the active compensation principle was based on changing the voltage applied to the piezo actuators in function of the change of the relative displacement of the active bearing surface (only an active geometrical compensation was applied). In this instance, only the thick bearing was tested with a static load of 600 N.

Results showed that the active compensation method works, increasing dynamic stiffness of the bearing in a high bandwidth (quasi-infinite static stiffness, fivefold increased at 50 Hz).

4. Summary and discussion

Passive and active compensation methods make it possible to ~~achieve significant~~ the air bearings performance and, in some cases, to obtain gains both in dynamic and static behaviours of air bearings. Passive compensation allows bearing performance to be only partially improved (infinite stiffness can be achieved over more than 20% of the bearing load range and up to a bandwidth of 5 Hz). On the other hand, active compensation, thanks to the integration of complex mechatronics systems (closed loop servo systems), is pushing the air bearing performance to their limits obtaining systems with wider working ranges where infinite stiffness and stability may be achieve. Currently available compensation methods were classified in three main categories on the basis of the modified control variable, e.g., the opening of a restrictor, the air gap shape and the air pad thickness. On the basis of table 1, active geometrical and in turn hybrid are those with the higher performance. In this table a dimensionless load capacity indicator $\bar{F}$ and the system bandwidth f_{max} are used in order to compare the reviewed compensation solutions. The type of the used actuator is another important aspect that has to be considered in designing active compensation system. The actuator choice ~~it~~ can significantly influence the performance of a compensation system, as it is possible to figure out from ~~the~~ table 6 where actuators features are reported. From this analysis it appears that, at the moment, piezo and magnetostrictive actuators guarantee the best performance concerning dynamics and power energy density ratio, but piezos are the most adopted for their relative low cost. On the other hand, magnetic actuators are currently used, especially in the large size applicasions, e.g.,linear slide, because can be very useful as preloading systems. It is worth noting that the air bearing preload has not a secondary aspect, since it was found that

higher preload makes it possible to have bearing with higher load capacity and stability [6]. The next step for this kind of application, as has already been made for journal bearings [31], [32] could be to employ the infrequently used active geometrical variation approach (3.2), for example by using PZT and flexure hinges, which are a well established pair in nano positioning. However, this is a slow process due to the extra expense and complexity of the mechatronic system and lack of experience in this area.

5. Conclusion

The paper presented an overview of compensation methods for aerostatic thrust bearings, distinguishing between passive and active compensation, and subsequently focusing on the latter one. Different active compensation methods were reviewed and categorized on the basis of a new classification criteria.
The pros and cons of each type of active compensation were analyzed and compared. The bearing load carrying capacities were compared on the basis of a dimensionless indicator which takes into account the bearing dimension (active surface), the supplied pressure P_s, the maximum load for obtaining infinite stiffness F_∞ and the relative working height of the air gap. The system bandwidth was used for comparing the dynamic performance of the different bearing prototypes. From here, it is possible to conclude that compensation methods based on hybrid and variation of the air gap shape make it possible to obtain air bearings with high dynamics, load capacity and stiffness. The next step for research in this field is to incorporate these systems into actual demanding ultra precision applications without excessive costs. The active compensation of aerostatic thrust bearings is still a challenging research field, and unexplored technical solutions and studies can contribute to further advances.

References

[1] Precision Engineering; vol. 14. 1992. ISBN 0-07-154828-9. doi:10.1016/0141-6359(92)90202-8.

[2] Belforte G, Raparelli T, Viktorov V, Trivella a. Discharge coefficients of orifice-type restrictor for aerostatic bearings. Tribology International 2007;40(3):512–21. doi:10.1016/j.triboint.2006.05.003.

[3] Fourka M, Tian Y, Bonis M. Prediction of the stability of air thrust bearings by numerical, analytical and experimental methods. 1996. doi:10.1016/0043-1648(95)06782-5.

[4] Al-Bender F. On the modelling of the dynamic characteristics of aerostatic bearing films: From stability analysis to active compensation. Precision Engineering 2009;33(2):117–26. URL: http://www.sciencedirect.com/science/article/pii/S0141635908000883. doi:http://dx.doi.org/10.1016/j.precisioneng.2008.06.003.

[5] Snoeys R, Al-Bender F. Development of improved externally pressurized gas bearings. KSME Journal 1987;1(1):81–8. URL: http://dx.doi.org/10.1007/BF02953383. doi:10.1007/BF02953383.

[6] Aguirre G, Al-Bender F, Brussel HV. A multiphysics model for optimizing the design of active aerostatic thrust bearings. Precision Engineering 2010;34(3):507–15. URL: http://www.sciencedirect.com/science/article/pii/S014163591000005X. doi:http://dx.doi.org/10.1016/j.precisioneng.2010.01.004.

[7] Talukder HM, Stowell TB. Pneumatic hammer in an externally pressurized orifice-compensated air journal bearing. Tribology International 2003;36(8):585–91. URL: http://www.sciencedirect.com/science/article/pii/S0301679X02002475. doi:http://dx.doi.org/10.1016/S0301-679X(02)00247-5.

[8] Blondeel E, Snoeys R, Devrieze L. Dynamic Stability of Externally Pressurized Gas Bearings. Journal of Lubrication Technology 1980;102(4):511–9. URL: http://dx.doi.org/10.1115/1.3251588.

[9] Bryant MR, Velinsky SA, Beachley NH, Fronczak FJ. A Design Methodology for Obtaining Infinite Stiffness in an Aerostatic Thrust Bearing. Journal of Mechanisms, Transmissions, and Automation in Design 1986;108(4):448–53. URL: http://dx.doi.org/10.1115/1.3258753.

[10] Plessers P, Snoeys R. Dynamic Stability of Mechanical Structures Containing Externally Pressurized Gas-Lubricated Thrust Bearings. Journal of Tribology 1988;110(2):271–8. URL: http://dx.doi.org/10.1115/1.3261598.

[11] Holster PL, Jacobs JAH. Theoretical analysis and experimental verification on the static properties of externally pressurized air-bearing pads with load compensation. Tribology International 1987;20(5):276–89. URL: http://www.sciencedirect.com/science/article/pii/0301679X87900284. doi:http://dx.doi.org/10.1016/0301-679X(87)90028-4.

[12] Chen MF, Lin YT. Dynamic Analysis of the X-shaped Groove Aerostatic Bearings with Disk-Spring Compensator. JSME International Journal Series C 2002;45:492–501. doi:10.1299/jsmec.45.492.

[13] Sato Y, Maruta K, Harada M. Dynamic Characteristics of Hydrostatic Thrust Air Bearing With Actively Controlled Restrictor. Journal of Tribology 1988;110(1):156–61. URL: http://dx.doi.org/10.1115/1.3261556.

[14] Huber JE, Fleck NA, Ashby MF. The selection of mechanical actuators based on performance indices. 1997. doi:10.1098/rspa.1997.0117.

[15] Niezrecki C, Brei D, Balakrishnan S, Moskalik A. Piezoelectric Actuation: State of the Art. The Shock and Vibration Digest 2001;33(4):269–80. doi:10.1177/058310240103300401.

[16] Mizumoto H, Matsubara T, Yamamoto H, Okuno K, Yabuya M. An Infinite-stiffness Aerostatic Bearing with an Exhaust-control Restrictor. In: Seyfried P, Kunzmann H, McKeown P, Weck M, editors. Progress in Precision Engineering. Springer Berlin Heidelberg. ISBN 978-3-642-84496-6; 1991, p. 315–6. URL: http://dx.doi.org/10.1007/978-3-642-84494-2_35. doi:10.1007/978-3-642-84494-2_35.

[17] MIZUMOTO H, SHIMIZU T. An Infinite-Stiffness Aerostatic Spindle with Active Restrictors. Journal of the Japan Society for Precision Engineering 1993;59(4):607–12. doi:10.2493/jjspe.59.607.

[18] Morosi S, Santos IF. Active lubrication applied to radial gas journal bearings. Part 1: Modeling. Tribology International 2011;44(12):1949–58. URL: http://www.sciencedirect.com/science/article/pii/S0301679X1100226X. doi:http://dx.doi.org/10.1016/j.triboint.2011.08.007.

[19] Morosi S, Santos I. From Hybrid to Actively-Controlled Gas Lubricated Bearings Theory and Experiment. Ph.D. thesis; 2011.

[20] Mizumoto H, Arii S, Kami Y, Goto K, Yamamoto T, Kawamoto M. Active inherent restrictor for air-bearing spindles. Precision Engineering 1996;19(23):141–7. URL: http://www.sciencedirect.com/science/article/pii/S0141635996000414. doi:http://dx.doi.org/10.1016/S0141-6359(96)00041-4.

[21] Mizumoto H, Arii S, Yabuta Y, Kami Y, Tazoe Y. Active Aerostatic Bearings for Ultraprecision Applications. In: Hinduja S, Fan KC, editors. Proceedings of the 35th International MATADOR Conference. Springer London. ISBN 978-1-84628-987-3; 2007, p. 289–92. URL: http://dx.doi.org/10.1007/978-1-84628-988-0_65. doi:10.1007/978-1-84628-988-0_65.

[22] Houqing Z, Jianguo L, Xiurong W, Yanhong X, Hongping Z. Applications

of Terfenol-D in China. Journal of Alloys and Compounds 1997;258(12):49–52. URL: http://www.sciencedirect.com/science/article/pii/S0925838897000686. doi:http://dx.doi.org/10.1016/S0925-8388(97)00068-6.

[23] Huang KY, Shiao YC. Design and development of magnetostrictive actuating restrictor for aerostatic thrust bearing. In: 12th IFToMM World Congress. 2007, p. 18–21.

[24] Schweitzer G. Active magnetic bearings-chances and limitations. In: IFToMM Sixth International Conference on Rotor Dynamics, Sydney, Australia; vol. 1. 2002, p. 1–14.

[25] Ro SK, Kim S, Kwak Y, Park CH. A linear air bearing stage with active magnetic preloads for ultraprecise straight motion. Precision Engineering 2010;34(1):186–94. URL: http://www.sciencedirect.com/science/article/pii/S0141635909000865. doi:http://dx.doi.org/10.1016/j.precisioneng.2009.06.010.

[26] Belforte G. Manuale di pneumatica. Automazione industriale; Tecniche Nuove; 2005. ISBN 9788848105415. URL: https://books.google.it/books?id=7mU6ngEACAAJ.

[27] Russell GW. Air bearing control system. 1994. URL: http://www.google.com.au/patents/US5347723.

[28] Raparelli T, Viktorov V, Manuello Bertetto A, Trivella A. Air bearing with pneumatic active control. In: Proceedings of the first 2000 AIMETA International Tribology Conference. 2000, p. 693–700. URL: http://porto.polito.it/1506694/.

[29] Belforte G, Raparelli T, Viktorov V, Trivella A. Analysis of steady and transient characteristics of pneumatic controlled air bearing. In: 5th JFPS International Symposium on Fluid Power. S. Yokota; 2002,URL: http://porto.polito.it/1506704/.

[30] Aguirre G, Al-Bender F, Van Brussel H. A multiphysics coupled model for active aerostatic thrust bearings. In: Advanced Intelligent Mechatronics, 2008. AIM 2008. IEEE/ASME International Conference on. 2008, p. 710–5. doi:10.1109/AIM.2008.4601747.

[31] HORIKAWA O, SHIMOKOHBE A. An Active Air Bearing : Control of Radial Axis Motion and Stiffness. JSME international journal Ser 3, Vibration, control engineering, engineering for industry 1990;33(1):55–60. doi:10.1299/jsmec1988.33.55.

[32] Shimokohbe A, Horikawa O, Sato K, Sato H. An Active Air Journal Bearing with Ultraprecision, Infinite Static Stiffness, High Damping Capability and New Functions. {CIRP} Annals - Manufacturing Technology 1991;40(1):563–6. URL: http://www.sciencedirect.com/science/article/pii/S000785060762054X. doi:http://dx.doi.org/10.1016/S0007-8506(07)62054-X.

Figures

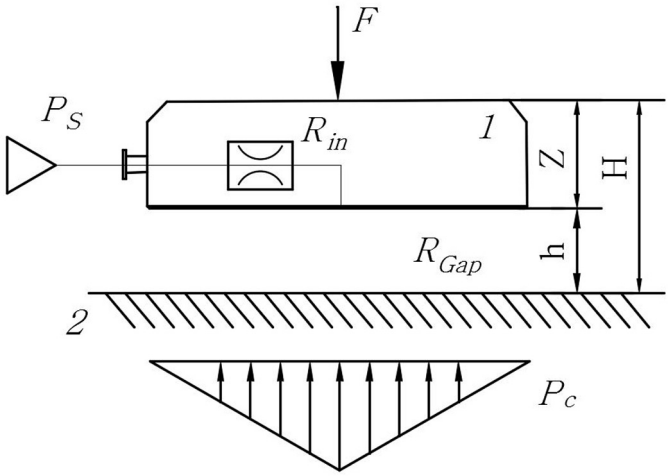

Figure 1: A schematic representation of an ATB: air gap width h, ATB thickness Z, controlled height H, air gap pressure distribution P_c, internal flow resistance R_{in}, air gap flow resistance R_{Gap} and external load F.

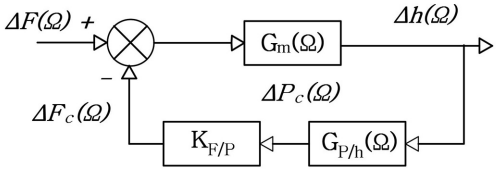

(a) Block diagram of conventional ATB.

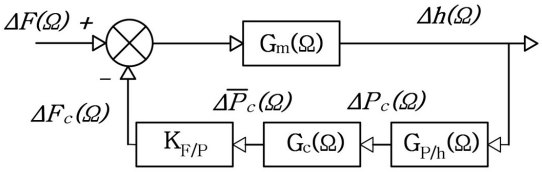

(b) Block diagram of an inherent compensated passive air pad.

Figure 2: Block diagrams of passive air pads.

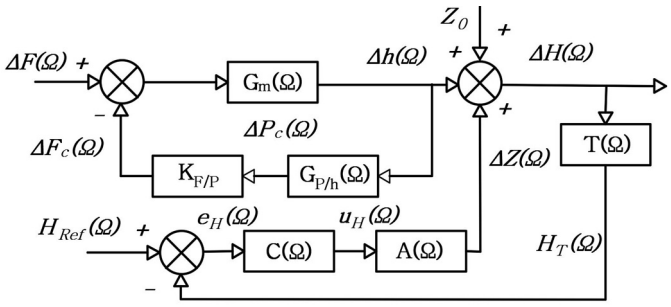

Figure 3: Block diagram of the active compensation by changing the air gap width h and with indirect H measurements.

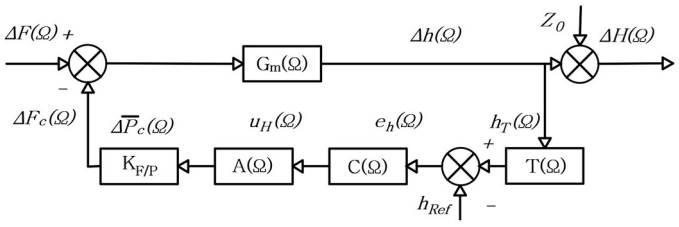

Figure 4: Block diagram of the active compensation by changing the air pad thickness Z with a direct measurement of H.

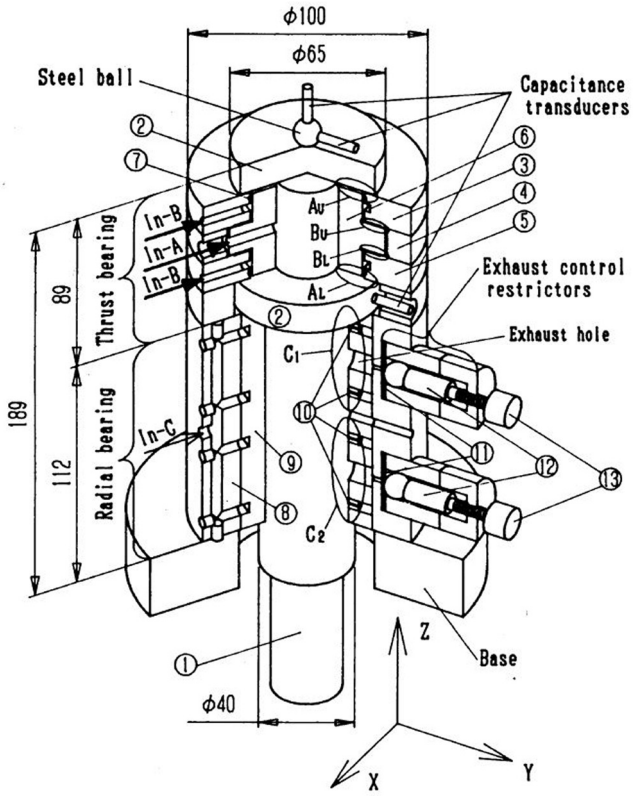

Figure 5: An infinite-stiffness aerostatic spindle: shaft 1, thrust plate 2, outer ring 3, outer ring 4, outer ring 5, restriction ring 6, o-ring 7, outer sleeve 8, inner sleeve 9, inflow restrictor 10, diaphragm 11, piezoelectric actuator 12, adjusting screw 13 (from [17]).

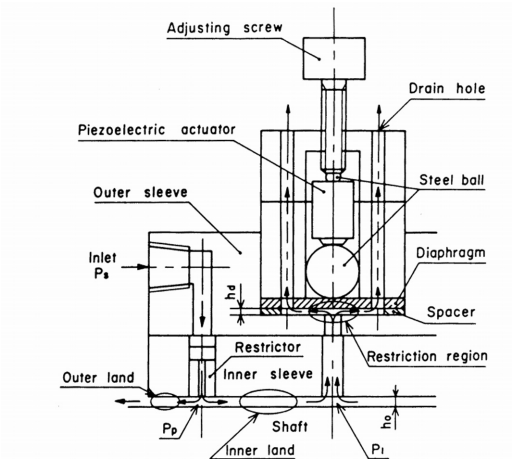

(a) Magnified view of ECR restrictor (from [17]).

(b) Operating principle of ECR (from[17])

Figure 6: ECR from [17].

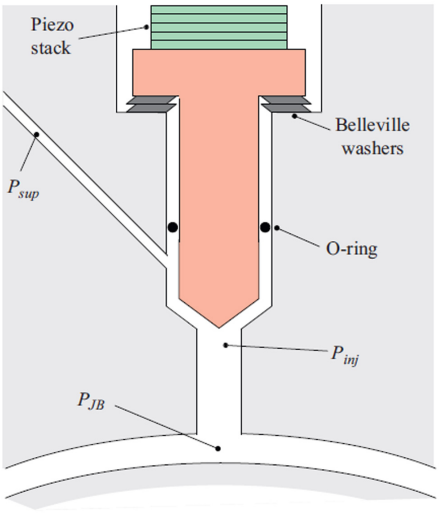

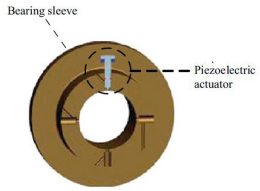

(a) The injection system designed by Morosi et al. (from [19]).

(b) 3D view of the piezoelectric injection system (from [19]).

Figure 7: The hybrid journal bearing by morosi et al. (from [19]).

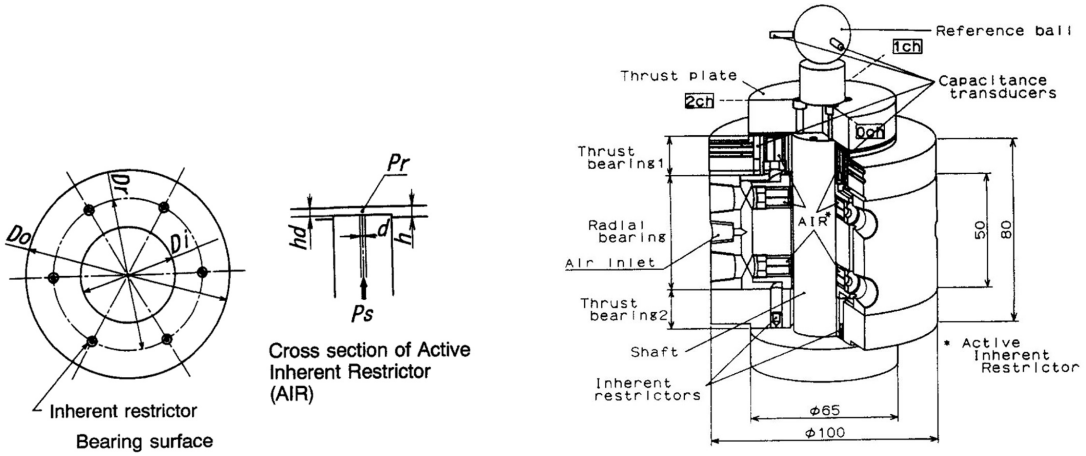

(a) An annular pad aerostatic bearing with the AIR (from [20]).

(b) Schematic view of an air bearing spindle with AIRs (from [20]).

Figure 8: AIR from [20].

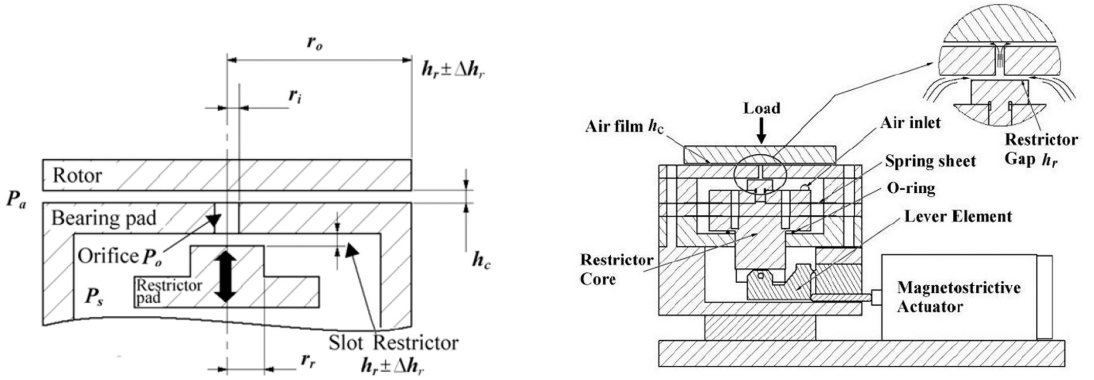

(a) Active compensation by means of a slot restrictor (from [23]).

(b) Construction of active compensation restrictor (from [23]).

Figure 9: Magnetostrictive actuating restrictor.

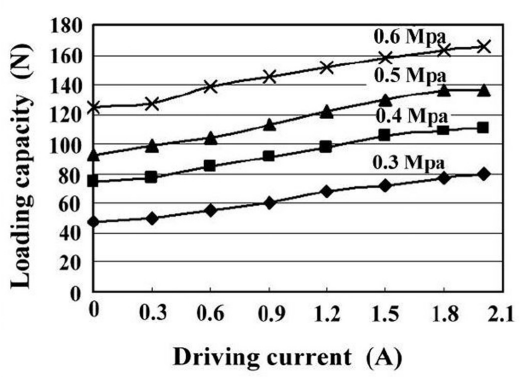

Figure 10: Influence of driving current and supply pressure on loading capacity for an air-film thickness of 10 μm (from [23]).

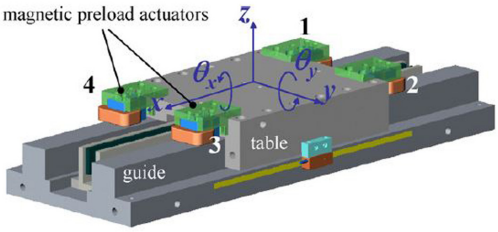

(a) A schematic view of the AC system by using valves (from [29]).

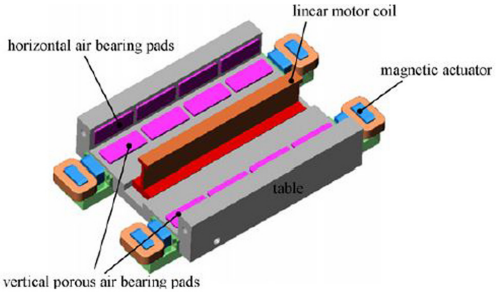

(b) The bottom view of the linear air bearing stage (from [25]).

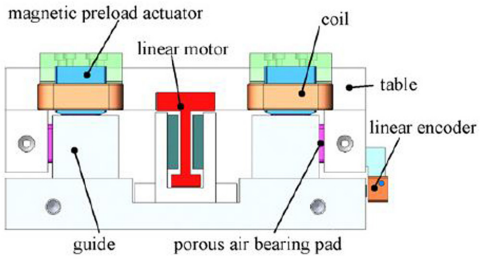

(c) Front view of the linear air bearing stage (from [25]).

Item	Specifications
Air bearing pad size ($Lx \times Ly \times H$)	$50 \times 20 \times 5$ mm^3
Air bearing clearance (vertical)	13.5 μm
Vertical air bearing stiffness	38.5 N/μm
Required preload (vertical)	250 N
Permanent magnet size	$25 \times 8 \times 4$ mm^3
Table weight	10.0 kg
Magnetic preload	35.8×4 N
Current gain of an actuator	15.5 N/A

(d) Specifications (from [25])

Figure 11: An air bearing stage with active magnetic preload (from [25]).

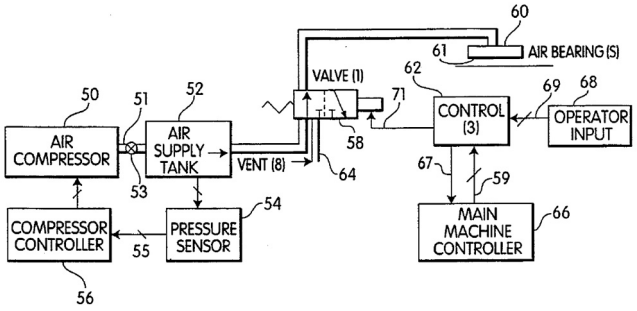

Figure 12: The scheme of the control system designed by G. Russel (from [27]).

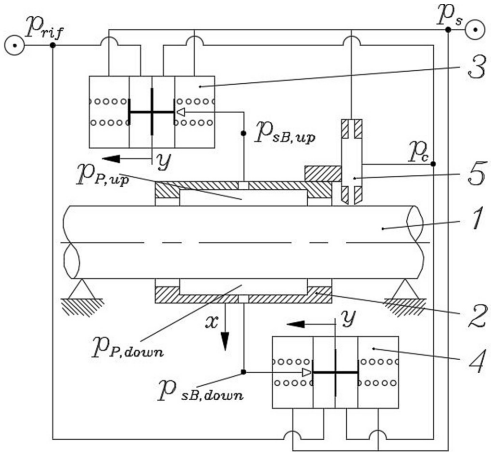

(a) A schematic view of the AC system by using valves (from [29]).

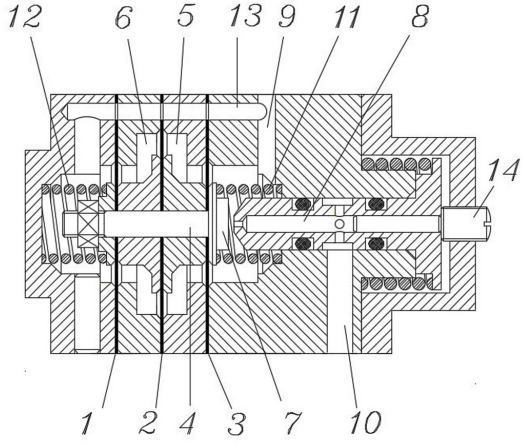

(b) Valve longitudinal cross section (from [29]).

Figure 13: An active compensation method by means of pneumatic valves.

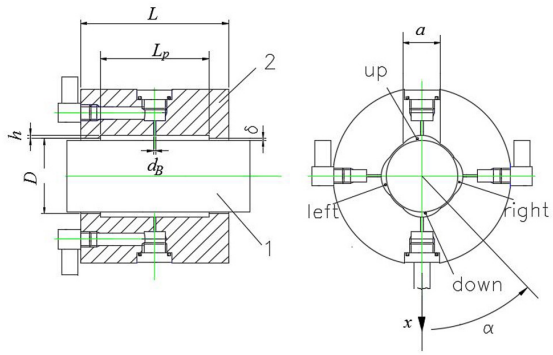

Figure 14: The pneumostatic journal bearing (from [29]).

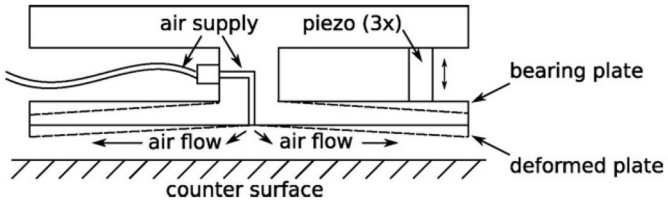

Figure 15: Sketch of the active aerostatic bearing with a conicity control (from [6]).

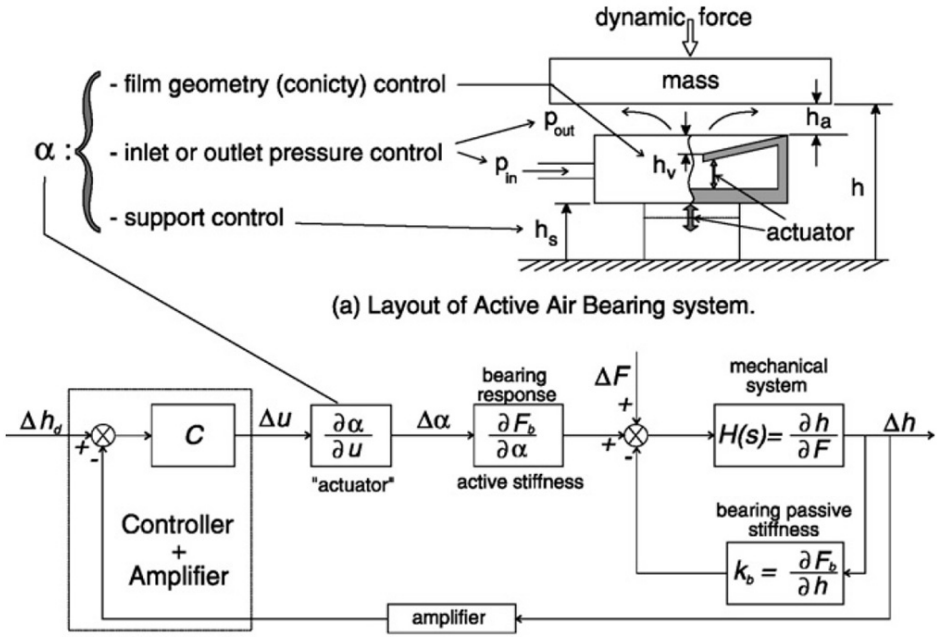

Figure 16: Schematic of the active bearing system: (a) layout of active air bearing system and (b) schematic of the active compensation system (from [4]).

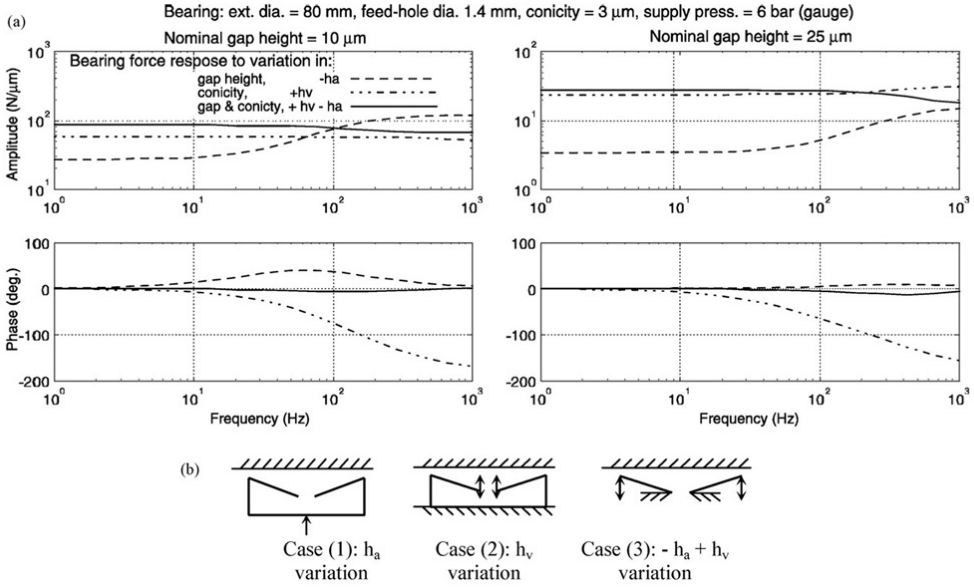

Figure 17: Bearing force response to variation in gap height, conicity and their combination (from [4]).

Tables

Table 3: Comparison between active and passive compensation characteristics.

Compensation type	**Advantages**	**Disadvantages**
Passive compensation	-cheaper	-infinite stiffness for maximum 20% of the load range -lower dynamic range
Active compensation	-higher dynamic range -higher accuracy -possible integration of monitoring systems	-more expensive

Table 4: Comparison among some of the reviewed active compensation strategies: $\bar{F} = \frac{F_\infty \cdot h_0}{P_S \cdot S \cdot h}$ dimensionless load capacity indicator

Reference	$\bar{F} \cdot 10^{-3}$ **[-]**	**Bandwidth [Hz]**	**Categorization**	**Actuator**
H. Mizumoto et al. [17]	10.15	50	A.F. (Exhaust)	PZT
H. Mizumoto et al. [21]	46.90	Static	A.F. (Air gap)	PZT
K.Y. Huang et al. [23]	99.00	Static	A.F. (Air gap)	Magnetostric.
S.K. Ro et al. [25]	Finite stiffness	Static	A.F. (Air gap)	Elecromagn.
T. Raparelli et al. [29]	29.47	Static	A.F. (Air gap)	Valve
F. Al Bender et al. [4],[30]	198.90	300	Hybrid	PZT

Table 5: Comparison of the performance of different kind of actuators used in active compensation [14].* The dimensionless stroke work coefficient was defined as the ratio of the maximum work done in a single stroke to the maximum work per unite volume ($\sigma_{max} \cdot \epsilon_{max}$).

Actuator type	**maximum frequency** $[s^{-1}]$	**maximum power density** $[Wm^{-3}]$	**efficiency** η [-]	**strain resolution** [-]	**work stroke coefficient*** [-]
PZT	10^5 – $3 \cdot 10^7$	$9 \cdot 10^7$ – $3 \cdot 10^8$	0.9 – 0.99	10^{-9} – $3 \cdot 10^{-7}$	$\simeq 0.5$
Magnetostrictor	$\simeq 3 \cdot 10^7$	10^8 – $7 \cdot 10^8$	0.8 – 0.99	10^{-7} – 10^{-6}	$\simeq 0.5$
Magnetic	5 - $5 \cdot 10^4$	10^4 – 210^6	0.5 – 0.8	10^{-6} – $2 \cdot 10^{-2}$	0.5 – 1
Pneumatic	50 – 300	$5 \cdot 10^6$	0.3 – 0.4	10^{-5} – $2 \cdot 10^{-4}$	$\simeq 1$

Table 6: Comparison of the performance of different kind of actuators used in active compensation [14].

Actuator type	**Advantages**	**Disadvantages**
PZT	-high dynamics -high efficiency -high power density -high resolution	-low stroke work -auxiliary control equipment need -hysteresis -non linearity -typically brittle
Magnetostrictive	-high power density -non contact actuation -high dynamics -high efficiency -medium resolution -medium actuation strain	-auxiliary control equipment -low stroke work -hysteresis -non linearity -typically brittle
Electromagnetic	-medium dynamics -medium efficiency -contactless actuation -medium stroke work -medium power density -medium resolution	-hysteresis -non linearity -auxiliary control equipment
Pneumatic valves	-cheap -medium power density -high stroke work -medium resolution -medium power density	-hysteresis -non linearity -leaks -low efficiency -low dynamics -noise